On the Use of Complex Excitation Sequences for Eddy Current Testing

Giovanni Betta[1], Pietro Burrascano[2], Luigi Ferrigno[1], Marco Laracca[1], Marco Ricci[2] and
Giuseppe Silipigni[2,3]

[1] *University of Cassino, Via G. Di Biasio, 43, Cassino, Italy, +3907762993673, betta@unicas.it*
[2] *University of Perugia, 05100, Pentima Bassa, 4, Terni, Italy +390744492937, pietro.burrascano@unipg.it*
[3]*University of Messina, 98166, Contrada di Dio, 1, Messina, Italy*

Abstract- Eddy Current Testing (ECT) is a Non Destructive technique widely used in many industrial application fields in which it is very important to detect the presence of thin defects (generally called cracks) in conductive materials. Features of this technique are the cost-effective implementation and the kind of retrieved measured data that make possible estimating geometrical characteristics of a crack as position, length, width and depth. The analysis of these characteristics allows the user to accept or discard realized components then improving the production chain. To accomplish for this task some aspects have to be taken into account during the measurement process. They mainly concern with the realization of suitable measurement setup and post processing stages. As far as the measurement setup is concerned, crucial aspects are the choice of measurement and excitation devices. As for the former, in the past years the literature deeply explored many types of measurement probes highlighting advantages and disadvantages of different solutions. The choice of optimized excitation devices and strategies is now interesting recent studies about Non Destructive ECT (ND-ECT): together with common aspects as the amplitude and the frequency of the exciting signal, recently the attention has been paid to issues as the type of signal to be adopted. In particular it has been found as the use of complex excitation signals, meant as signals different from the sinusoidal ones and with wide frequency content, might raise eddy current responses trying to support the measurement, detection and characterization stages when "difficult cases" are explored (i.e. very short or annealed cracks). In this paper the authors propose an experimental comparison of different excitation signal designed to improve the quality of experimental data when difficult cases are experienced (such as annealed and small cracks) and consequently to obtain a more reliable extraction of defects geometrical features.

I. Introduction

The use of ECT is probably one of the most widespread electromagnetic techniques for the inspection of conductive materials [1]. It allows the detection, the location, and the characterization of the geometrical characteristics of defects with relatively low cost and simple hardware set-up. Even if the physical principle that lies upstream of the technique of ECT is very simple, its use for crack characterization purpose rather than for the only crack detection is a key issue in literature. In fact, many aspects have to be taken into account and suitably optimized during the overall measurement process. They mainly concern with the realization of suitable measurement setup and post processing stages.

With respect to the measurement setup, the choice and the performance of measurement and excitation devices are of utmost importance. As for the former aspect, in the last years the literature have deeply explored physical principles and manufacturing techniques with the aim of realizing very good eddy current sensors and probes. Technologies as those based on coils, fluxgate, fluxset, Giant Magneto Resistance (GMR), hall effect and so on, have been analysed and adopted to realize ECT instruments.

As far as the latter aspect is concerned, recent studies are involved in finding excitation solutions able to promote the measurement process. In this scenario, a key ingredient of the measurement process is the choice of signal type, frequency and amplitude to be adopted in the excitation stage. The criticality consists in finding excitation signals capable of causing sufficient amplitudes of eddy currents both for defects present on the surface of the material and for defects included in the material [2-4]. It is here reminded that the depth of eddy current is determined by the exciting frequency in such a way that the lower frequencies penetrate deeper than the higher ones, but, at the same stages, the lower the frequency the lower the amplitude of the reaction signal at the measurement probe. Suitable excitation signals are therefore required in order to achieve a compromise between the need of discover and characterize sub superficial defects and the need of obtaining good signal to noise ratio and repeatability of the measurement signals. In force of these considerations, the actual research on ECT is considering excitation signals containing wideband spectrums instead of the sinusoidal ones. To this aim some emerging techniques based on the use of multi-Frequency, pulsed, chirp, and pseudo-noise signals to cite a few are proposed in literature as alternatives to traditional ECT signals in order to, primarily, improve the sensitivity
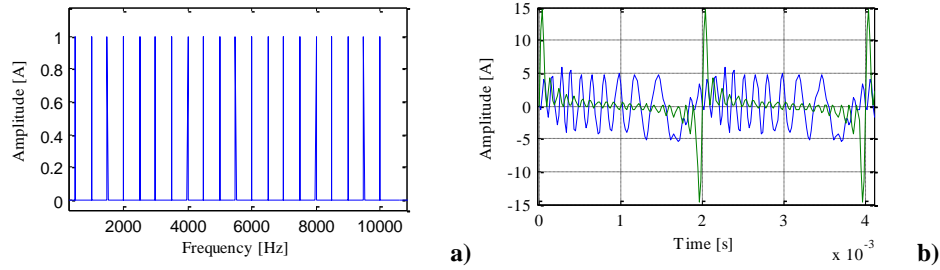
Figure 1. Example of a multisine signal considering 20 sinusoidal tones. (a) Frequency displacement of the considered tones; (b) Time signal with (blue line) and without (green line) the phase optimization.

of defect detection in some particular application field, and especially for small cracks, embedded deep in layered components [2-8]. Each one of these considered excitation signals present advantages and disadvantages that prevent the election of an absolute best excitation signal. The authors have engaged this field proposing probes, measurement methods and excitation strategies to optimize the defect characterization by ECT methods [2-4, 7-11]. In this paper they present an experimental study aimed in comparing different excitation strategies for the assessment of the above-mention characteristics of thin cracks in conductive materials. In particular, the paper proposes an experimental approach based on the definition and analysis of a suitable figure of merit related to the detection capability. The final aim of the proposed study is toward the realization of a FPGA-based smart ECT-based measurement instrument able to automatically find the best excitation strategy depending on the defect characteristics [12].

II. Theoretical Background

Some ECT excitation strategies are experimentally analysed and compared in this paper. They concern with the use of multi-frequency and chirp signals.

A. Multi-Frequency Signal

A multi-frequency signal is realized combining some sinusoidal tones in order to excite the desired frequency components with the desired amplitudes. The general formulation of a multi-sine signal is given hereafter.

$$I(t) = \sum_{k=1}^{Ns} I_k * \sin(2 * pi * f_k * t + \phi_k) \qquad (1)$$

where I_k is the current amplitude of the k-th sinusoid, f_k and ϕ_k are respectively the frequency and the phase of the k-th sinusoid and Ns is the number of considered tones.
With a proper choice of ϕ_k,

$$\phi_k = -\pi * \frac{k(k-1)}{N_s} \qquad (2)$$

the resulting excitation exhibits a quite constant envelope, which is desirable for optimizing the power delivered to the exciting probe. Figure 1a) shows an example of multi-frequency signal composed of 20 tones up to 10 kHz and with equal amplitudes. Looking at Figure 1b), it is possible to highlight the effect of the phase optimization on the maximum values of the multi-sine signal. In addition, it is evident that the higher the number of tones the better are the information retrieved from the eddy currents on the specimen. On the other hand, the higher the number of tones, the higher the total root mean square value of the generated signal. If this value is too high problems related to the excitation coil heating and the power supply dimensioning arise. For these reasons generally a finite number of tones is suitably chosen. Useful considerations concerning with the relationships between the adopted frequencies and the specimen depth might drive the choice of tone number, frequencies and amplitudes.

B. Chirp Signal

By tuning the amplitudes I_k and the phases ϕ_k, multi-tone signals can be generated in order to follow an arbitrary power spectrum while minimizing the peak factor, as said. In the case of N_S different harmonically related frequencies with constant power for each tone, the phases ϕ_k are derived from the continuous phase function of linear frequency modulated signals, i.e. from a Linear Chirp signal [13].
The Linear Chirp signal is one of the most used waveform used in pulse compression applications such as radar,

Linear range [G]		Sensitivity [a] [mV/V/G]		Non Linearity	Hysteresis [b]	Supply voltage [V]		Saturation field
min	max	min	max	[%]	[%]	min	max	[G]
0.6	3.0	11	18	6	15%	±1	±12	6
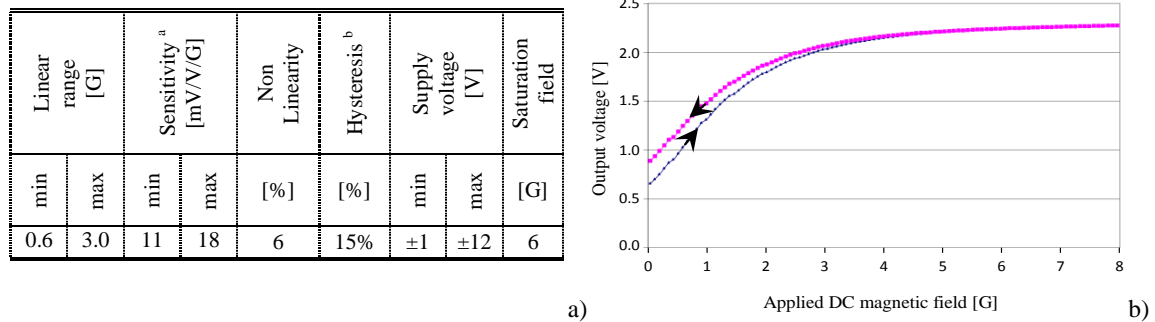
Figure 2. Main characteristics of the adopted GMR sensor (a), and behavior of the unipolar input output characteristic(b). A temperature equal to T=22.5 °C and a power supply equal to 5 V DC are considered.

sonar, spread-spectrum communications, etc. and it is described by the general expression:

$$s(t) = \alpha(t)\sin(\Phi(t))) \text{ where } \Phi(t) = 2\pi(f_1 t + \tfrac{f_2 - f_1}{2T} t^2) \qquad (3)$$

is a quadratic phase term ensuring a linear varying instantaneous frequency $f_i(t) = \frac{1}{2\pi}\frac{d\Phi}{dt} = f_1 + \frac{f_2 - f_1}{T}t$. $\alpha(t)$ is a windowing function that is not-vanishing only in the interval $t Î [0,T]$, and in the present case was chosen rectangular, i.e. $\alpha(t) = \theta(t) - \theta(t - T)$, in order to ensure a constant envelope and an almost flat power spectrum in the frequency range $f Î [f_1, f_2]$. More generally, $\alpha(t)$ can be used to modulates the amplitude of s(t) and, due to the characteristic of linear chirp, also the power spectrum.

By replacing the multi-tone signal with a chirp one, a continuous frequency range can be excited providing potentially a better resolution in evaluating the more sensitive inspection frequency for a given defect. Nevertheless, also the number of tones can be increased in the multi-tone signal to guarantee the wanted resolution so that the main advantage of the chirp excitation actually does not lie in its continuous frequency range of excitation but indeed is represented by the possibility to characterize contextually the time- and the frequency-domain response of the sample. In particular, besides of reconstructing the transfer function H(ω) in the frequency range of interest, the impulse response h(t) of the sample can be retrieved by using a pulse-compression procedure. Since it was found that time- and frequency- analysis can provide complementary information about defects and moreover they are differently affected by the possible noise sources (environmental, lift-off variation, etc), the contextual analysis can improve the defect detection capability.

III. Experimental Setup

In the following details about the adopted ECT probe together with a description of the measurement setup are given. The ECT probe is based on the use of a GMR sensor arranged in a Wheatstone bridge configuration [3,14]. Figure 2a) shows its main features while Figure 2b) show the unipolar input/output characteristic.

The sensor has been arranged in the measurement setup sketched in Figure 3. It can be divided into generation and measurement sections. The generation section comprises the 20-20 Kepko[TM] Bipolar Operational Amplifier (AMP) driven by a frequency generator (GEN) and the exciting coil. The measurement section comprises: (i) the Agilent[TM] 34401A digital multimeter (MULT1) that measures both the AC and DC currents flowing in the exciting coil; (ii) the Analog Devices[TM] AD620 instrumentation amplifier, with a fixed gain equal to 10, whose output is measured by the Agilent[TM] 34401A digital multimeter (MULT2) that allows AC and DC voltage output of
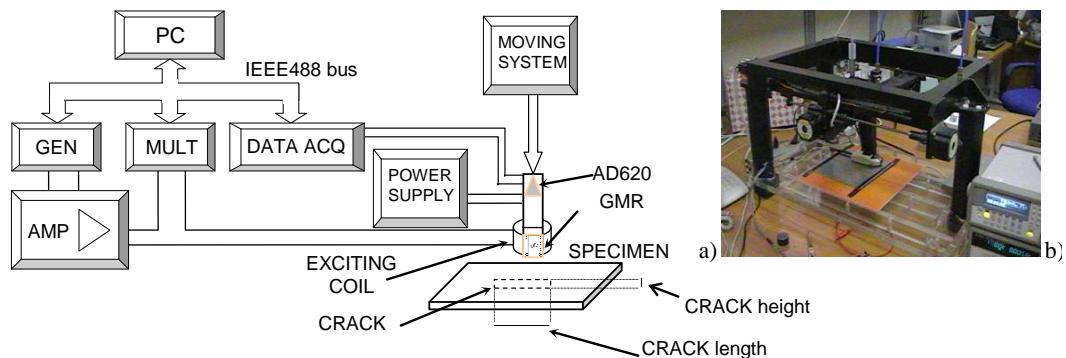
Figure 3. The developed measurement station (a), and a photo that highlights the precision moving system (b).

Table I. Geometrical characteristics of the adopted specimen; each crack has a width equal to 0.1 mm

Crack characteristics	Sample				
	#1	#2	#3	#4	#5
Length [mm]	1,0	5,0	5,0	5,0	8,0
Height [mm]	1,0	1,6	1,0	0,4	1,0
Depth [mm]	1,0	0,4	1,0	1,6	1,0

the sensor to be measured; (iii) a data acquisition system (DATA ACQ) based on the National Instruments™ NI USB 6212 allows the data storage for the post-processing stage; (iv) a Keithley™ 2700 digital multimeter (MULT3), fed by a K-type thermocouple, that monitors the GMR temperature. The whole measurement station is driven through a personal computer (PC) running an automation software written in the LabView™ 7.1 environment. This software is able to generate the numerical multi-sine and chirp signals, to load the signals on the function generator and to acquire data from all the measurement devices present in the setup. Finally a precision moving system moves the probe on the specimen following the selected path with a mean precision of 0.1mm. In particular the data are collected on a regular grid of points of 31 x 41 mm with a scanning path of 1 mm.

All the experimental tests have been carried out on specimens with known defects. All the specimens are plates realized in the 2024-T3 aluminum alloy. They are square plates characterized by a length 20 cm and thicknesses equal to 2 mm. The thin defect is located at the center of each plate. Each defect has a width equal to 0.1 mm. Details on each specimen are reported in Table I. A total of 5 specimens have been analyzed.

IV. Results

A. Post processing for the multi-frequency signals

Different post-processing algorithms have been applied for the multi-sine and chirp signals. As for the former the voltage proportional to the reaction magnetic field acquired by the ECT probe has to be processed in order to extract the material response to the multi-frequency stimulus. A Goertzel based algorithm has been developed to estimate the field amplitude and phase values for each frequency component of the acquired signal. In this way an electromagnetic response of the material at different frequencies is obtained.

For each frequency $\{f_\alpha, \alpha \in [1,10]\}$ a 2D image that visualizes for each point $\{(x,y): x \in [1,41], y \in [1,31]\}$ the amplitude of the "normalized" transfer function $|\hat{H}(f_\alpha, x, y)| = |H(f_\alpha, x, y)/H(f_\alpha, 1, 1)|$ is formed. The normalization is made with respect to the transfer function measured on a healthy point of the sample (in this case the first scanned point). For each sample Ns=10 images are then obtained, henceforth labelled as IM_MTαkHz. A 2D band pass filter acting as noise smoothing in the region of interest is applied to reduce the effect of the environmental noise, thermal drifts in components and lift-off variation. It is worth noting that for small inner defects, the noise can be comparable with the signal then affecting the SNR of the data and of the images.

For example considering the Sample #4 and the exciting frequency of 7 kHz, figure 4 shows the effect of the filtering procedure. It is possible to highlight as the low frequency components corresponding to intensity variations drift are filtered out as well as high frequency components corresponding to the effect of AWGN. After the processing, the defects are therefore more visible.

B. Post processing for the chirp signals

To extract the data of interest from the acquired chirp signal different strategies can be implemented. The authors
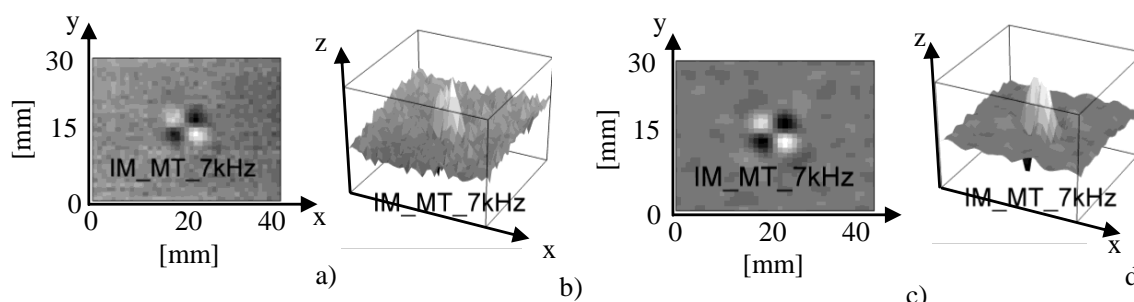
Figure 4. (a) Normalized image for the multi-frequency stimulus at the exciting frequency of 7 kHz; (b) map of the same image inthe xyz space; (c) effect of the bandpass filtering procedure in the image sketched in (a), and (d) map in the xyz space of the filtered image.
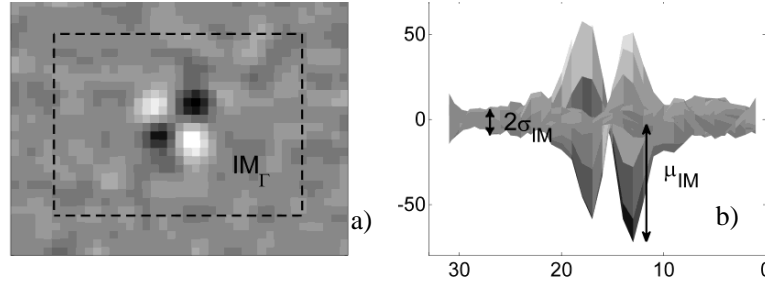
Figure 5. The selected figure of merit. The region of interest (a), and meaning of the σ_{IM} and μ_{IM} parameters (b).

have explored three different strategies that are described in the following.

i) For each point (x,y) the modulus of the "normalized" transfer function $\left|\hat{H}(f,x,y)\right| = \left|H(f,x,y)/H(f,1,1)\right|$ is calculated and subdivided in Ns=10 adjacent frequency regions each of them centred at the tone f_α with $\alpha \in [1,10]$. Then, similarly to the multitone case, for each sample Ns =10 images are obtained, henceforth labelled as IM_CH_αkH. For each image, at each pixel corresponds the maximum of the normalized transfer function in the α–th bin:

$$IM\_CH\_\alpha kHz(x,y) = max_f \{|\hat{H}(f,x,y)|, f \in [\alpha kHz - \Delta, \alpha kHz + \Delta]\} \quad (4)$$

In this case 2Δ=1kHz is the bin width.

ii) For each point (x,y) the "normalized" impulse response $\hat{h}(t,x,y) = h(t,x,y) - h(t,1,1)$ is calculated by applying pulse compression. The image IM_CH_T is then formed by taking for each point the maximum of the impulse response:

$$IM\_CH\_T(x,y) = max_t \{\hat{h}(t,x,y)\} \quad (5)$$

iii) For each point (x,y) the Chirp-Z-Transform $\hat{D}(f,x,y) = CZT[\hat{d}(t,x,y)]$ of the "normalized" output signal $\hat{d}(t,x,y) = d(t,x,y) - d(t,1,1)$ is calculated between $f \in [0.5kHz, 10.5kHz]$ and then the image IM_CH_F is formed by taking for each point the maximum of the Chirp-Z-Transform:

$$IM\_CH\_F(x,y) = max_f \{\hat{D}(f,x,y)]\} \quad (6)$$

While IM_CH_T and IM_CH_F are characteristic of the chirp since they exploit the continuous range of excitation frequencies, the IM_CH_f_α images deliberately resemble those derived by multitone signal in order to perform a more reliable comparison.

C. Selection of the figure of merit

Since the various images obtained exhibit different scales, depending on the various image formation algorithms, in order to fair evaluate and compare them, a scale-free figure of merit was defined and introduce based on an intuitive notion of "defect image quality". Precisely, for each image "IM" a SNR value was defined as:

$$SNR(IM) = \frac{max\{IM_\Gamma\} - mean\{IM_{\bar{\Gamma}}\}}{std\{IM_{\bar{\Gamma}}\}} = \frac{\mu_{IM}}{\sigma_{IM}} \quad (7)$$

where IM_Γ and $IM_{\bar{\Gamma}}$ are complementary parts of the image containing and not containing the defect respectively. In can be highlighted that the higher the SNR value, the cleared the defect effect and the higher the possibility to detect it. A graphic explanation of the proposed figure of merit is reported in Figure 5.

D. Preliminary results and comments

Table II. Results obtained for the selected figure of merit

SAMPLE	Multi-tone	Chirp with method i)	Chirp with method ii)	Chirp with method iii)
#1	10	12	13	12
#2	120	104	123	102
#3	52	65	57	52
#4	7	11	8	8
#5	71	63	70	64

Tests were carried out on the five samples described in section III are reported Table II. Some consideration can be made: i) the value of SNR depends on the values of length, depth and height of the crack; (ii) the type of chirp processing strongly affect SNR and it is not possible to identify a processing that is always the best; (iii) fixed the crack length; the chirp excitation signal seems to be more promising when short cracks (low values of l) are considered while multi-tone obtains better performance in the case of long crack; (iv) when the crack is small as for the depth or very annealed the chirp processed with the method iii obtains appreciable results (see rows of sample #3and #4);

V. Conclusions

The paper presented a preliminary experimental comparison between two of the most adopted complex excitation signals for ND-ECT. Tests were executed on a reliable measurement setup and on specimen with reference cracks representing very difficult cases (short and annealed cracks). The introduction of a suitable figure of merit allowed a preliminary quantitative comparison to be carried out. As expected it has been demonstrated that it is not possible to identify an excitation signal that is always the best [15]. In particular, different behaviors between multi-tone and chirp excitation signals are related to the geometrical dimensions of the crack. In addition, as for the chirp signal, also the processing strategy might leads to very different results. Future work will concern with the introduction of further figures of merit and analyses able to strictly relate the choice of the best excitation strategy with the crack characteristics with the final aim to implement an excitation method able to improve the crack detection and measurements.

Acknowledgment

References

[1]   D.C. Jiles, "Review of magnetic methods for non-destructive evaluation (Part 2)" NDT Int., vol. 23, pp. 83-92, 1990.

[2]   A. Bernieri, G. Betta, L. Ferrigno, M. Laracca, "Crack Depth Estimation by Using a Multi-Frequency ECT Method," IEEE Transactions on Instrumentation and Measurement, Vol. 62, Issue: 3, pp. 544-552, 2013

[3]   A. Bernieri, L. Ferrigno, M. Laracca, A. Tamburrino, "Improving GMR Magnetometer Sensor Uncertainty by Implementing an Automatic Procedure for Calibration and Adjustment," Proceeding of IMTC Conference, Warsaw, Poland, May 2007.

[4]   A. Bernieri, G. Betta, L. Ferrigno, M. Laracca, "Multi-Frequency Eddy Current Testing using a GMR Based Instrument," International Journal of Applied Electromagnetics and Mechanics, vol. 39, pp. 355-362, 2012

[5]   W. Yin, S J Dickinson and A J Peyton "A multi-frequency impedance analysing instrument for eddy current testing" Meas. Sci. Technol, vol. 17, pp. 393-402, 2006

[6]   Guang Yang et al., "Pulsed Eddy-Current Based Giant Magnetoresistive System for the Inspection of Aircraft Structures," IEEE Trans. Magn., Vol. 46, N. 3, pp. 910-917, March 2010.

[7]   P. Burrascano, M. Carpentieri, A. Pirani, M. Ricci "Galois sequences in the non-destructive evaluation of metallic materials", Meas. Sci. Technol, vol. 17, pp.2973-2979, 2006.

[8]   P. Burrascano, M. Carpentieri, A. Pirani, M. Ricci, F. Tissi, "Time domain deconvolution approach relying on Galois sequences", COMPEL: The International Journal for Computation and Mathematics in Electrical and Electronic Engineering, Vol. 26, Issue 2, pp.380-388, 2007

[9]   A. Pirani, M. Ricci, R. Specogna, A. Tamburrino, F. Trevisan,"Multi-frequency identification of defects in conducting media", Inverse Problems, vol. 24, 035011, 2008

[10]   A. Bernieri, L. Ferrigno, M. Laracca, M. Molinara, "Crack Shape Reconstruction in Eddy Current Testing Using Machine Learning Systems for Regression", IEEE Trans. Instrum. Meas., Vol. 57, n.9, pp. 1958-1968, 2008.

[11]   A. Bernieri, G. Betta, L. Ferrigno, M. Laracca, "A novel biaxial probe implementing multifrequency excitation and SVM processing for NDT", Proceeding of IEEE International Instrumentation and Measurement Technology Conference-I²MTC 2013, Minneapolis, MN, USA, pp. 284-289, May 2013.

[12]   L. Ferrigno, M. Laracca, C. Liguori, and A. Pietrosanto, "A FPGA-based Instrument for the Estimation of R, L, and C Parameters Under non Sinusoidal Conditions," IEEE Trans. Instrum. Meas., vol.61, n.5, pp. 1503-1511, 2012

[13]   M. R. Schroeder, "Synthesis of Low-Peak-Factor Signals and Binary Sequences With Low Autocorrelation", IEEE Transactions on Information Theory Vol. 16, Issue 1, pp. 85-89, 1970.

[14]   G. Betta, L. Ferrigno, M. Laracca, "GMR-based ECT Instrument for Detection and Characterization of Crack on Planar Specimen: a Hand-held Solution", IEEE Trans. Instrum. Meas., Vol. 61, No. 2, pp. 505-512, 2012

[15]   M. Morozov, G.Y. Tian, D. Edgar, "Comparison Of Pec And Sfec Nde Techniques", Nondestructive Testing and Evaluation Vol. 24, Iss. 1-2, 2009